

HIGH FIELD PERFORMANCE OF NANO-DIAMOND DOPED MgB_2 SUPERCONDUCTOR

Arpita Vajpayee, V.P.S. Awana, and H. Kishan

National Physical Laboratory, Dr. K.S. Krishnan Marg, New Delhi-110012, India

A.V. Narlikar

UGC-DAE Consortium for Scientific Research, University Campus, Khandwa Road, Indore-452017, India

G.L. Bhalla

Department of Physics and Astrophysics, Delhi University, New Delhi, India

X.L. Wang

ISEM, University of Wollongong, NSW 2522 Australia

Polycrystalline MgB_2 - $n\text{D}_x$ ($x=0$ to 0.1) samples are synthesized by solid-state route with ingredients of Mg, B and n -Diamond. The results from magneto-transport and magnetization of *nano*-diamond doped MgB_2 - $n\text{D}_x$ are reported. Superconducting transition temperature (T_c) is not affected significantly by x up to $x=0.05$ and latter decreases slightly for higher $x > 0.05$. $R(T)$ vs H measurements show higher T_c values under same applied magnetic fields for the *nano*-diamond added samples, resulting in higher estimated H_{c2} values. From the magnetization measurements it was found that irreversibility field value H_{irr} for the pristine sample is 7.5 Tesla at 4 K and the same is increased to 13.5 Tesla for 3-wt% $n\text{D}$ added sample at the same temperature. The $J_c(H)$ plots at all temperatures show that J_c value is lowest at all applied fields for pristine MgB_2 and the sample doped with 3-wt% $n\text{D}$ gives the best J_c values at all fields. For the pure sample the value of J_c is of the order of 10^5 A/cm² at lower fields but it decreases very fast as the magnetic field is applied and becomes negligible above 7 Tesla. The J_c is 40 times higher than pure MgB_2 at 10 K at 6 Tesla field in case of 3% $n\text{D}$ doped sample and its value is still of the order of 10^3 A/cm² at 10 Tesla for the same sample. On the other hand at 20K the

5%*n*D sample shows the best performance at higher fields. These results are discussed in terms of extrinsic pinning due to dispersed *n*-Diamond in the host MgB₂ matrix along with the intrinsic pinning due to possible substitution of C at Boron site and increased inter-band scattering for highly doped samples resulting in extraordinary performance of the doped system.

PACS: 74.70. Ad

Key words: nano- MgB₂, Flux pinning.

I. INTRODUCTION

The improvement of the pinning behavior in MgB₂ is being considered as a key issue in the superconductivity field; many attempts have been made in this direction for enhancing the pinning strength of MgB₂. In the last five years, various carbon sources [1-3], silicates [4], single elements [5,6], carbohydrates [7], organic acids [8] and other compounds [9,10] have been doped in MgB₂ and reported. It has become more clear that structural defects with dimensions at nano scale play an important role for flux pinning i.e. nanoparticle doping is the most effective approach to improve the superconducting performance of MgB₂ and making MgB₂ acceptable for practical applications [11]. Nano particle doping can modify structure and electronic properties such as T_c , upper critical field and its anisotropy, gaps width, inter and intra-band scattering, defect structure etc. [12-14]. In present paper, we are discussing the effect of *nano* diamond addition on polycrystalline MgB₂ i.e. how the superconducting performance of pristine sample is modified by addition of *n*-Diamond.

II. EXPERIMENTAL

The MgB₂-*nano* Diamond composites with composition MgB₂ - *n*D_x ($x= 0\%$, 1% , 3% , 5% , 7% & 10%) are synthesized by solid-state reaction route with ingredients of Mg, B and *n*-Diamond. The Mg powder used is from *Reidel-de-Haen* of assay 99%, B powder is amorphous and *Fluka* make of assay 95-97%. The *n*-Diamond powder is from Aldrich with average particle size (*APS*) of 7-10 nm. For synthesis of MgB₂-*n*D_x samples, the nominal weighed samples are ground thoroughly, palletized, encapsulated in soft iron tube and put in a quartz tube inserted in a programmable furnace under flow of argon at ambient pressure. The temperature of furnace is

programmed to reach 850 °C over 2 hours, hold at same temperature for two and half hours, and subsequently cooled to room temperature over a span of 6 hours in the same Argon atmosphere. The x-ray diffraction pattern of the compound was recorded with a diffractometer using $\text{CuK}\alpha$ radiation. SEM studies were carried out on these samples using a Leo 440 (Oxford Microscopy: UK) instrument. The magnetoresistivity, $\rho(T)H$, was measured with H applied perpendicular to current direction, using four-probe technique on *Quantum Design PPMS*. Magnetization measurements are carried out with a Quantum-Design *SQUID* magnetometer *MPMS-7*.

III. RESULTS AND DISCUSSIONS

X-ray diffractions patterns show that all the samples of MgB_2 - $n\text{D}_x$ series are of nearly single phase with only a small quantity of un-reacted MgO in them. For highest $n\text{D}_x$ sample, i.e., $x = 10\text{wt}\%$, the main intensity peak is broadened slightly (patterns not shown). The lattice parameters remain nearly invariant for all the samples until $x = 5\text{wt}\%$ for MgB_2 - $n\text{D}_x$. For 10 wt% sample, slight decrease in ‘ a ’ is seen. It means for this higher concentration some diamond particles has got broken into carbon atoms, which substituted at Boron site resulting in slight decrease in ‘ a ’ but at low concentration there is not such indication of breakage of n -Diamond.

Variation of resistance with temperature under applied magnetic fields up to 8 Tesla $R(T)H$ is shown in fig.1 (only transition zone). As we can see from this figure with increasing n -Diamond concentration, the superconducting onset temperature remains unchanged and the transition width changes slightly. This indicates that no substitution has taken place in this system. It is noted that $R(T)H$ curves for the doped samples shifted with increasing field much more slowly than the undoped one. For pure MgB_2 the $T_c(R = 0)$ value is observed at 38 and 18 K in zero and 8 Tesla applied fields respectively. Interestingly, the $T_c(R = 0)$ for MgB_2 -5wt% $n\text{D}$ sample in comparison to pure MgB_2 is lowered to 36 K in zero applied field, the same is increased to 22 K under 8 Tesla field.

Now, to see the effect of n -Diamond addition on the upper critical field H_{c2} , using resistivity variation under magnetic field plots we estimated the H_{c2} values i.e. H_{c2} obtained from the 90% values of the resistive transitions. The variation of H_{c2} with respect to temperature is not shown here (see Ref. 15), which demonstrates that on increasing the concentration of n -Diamond a clear shift in upper direction can be achieved. The behavior of 3-wt% & 5-wt% n -Diamond added samples is quite competitive; but since the T_c of 5% $n\text{D}$ is lower than 3% $n\text{D}$ so we can say

that 5%*n*D sample shows better improvement in H_{c2} value. The formation of nanodomains structures is due to the presence of dispersed diamond in parent MgB₂ grains (we have reported the HRTEM and ED pattern in another paper [15]) causing the disorder in lattice. These nanodomains, which are comparable in size (~ 8 to 10 nm) with the coherence length of MgB₂ could result in strong in-plane and out-of-plane scattering and contribute to the increase of H_{c2} value in a wide temperature regime.

In fig.2 the magnetic hysteresis loop for all the doped samples ($x = 0\%$, 1%, 3%, 5%, 7% & 10%) at 10K is shown in applied field up to 13 Tesla. This tells that the closing of hysteresis loop for pure MgB₂ is at ~ 6.5 Tesla whereas the same is opened up to ~11 Tesla for 3-wt% doped sample. This indicates that there will be significant improvement in irreversibility field values for the doped samples. The irreversibility fields (H_{irr}) is the one at which the magnetic hysteresis loop is nearly closed with $M \approx 0$. The H_{irr} versus x (concentration on *nano* diamond) plot is shown in inset of fig.2 at 4k, 10K & 20K. The best values of H_{irr} among these diamond added samples (MgB₂-*n*D_{*x*}) is found for the sample with $x=3\%$. The H_{irr} values for the undoped samples are 7.5, 6.5 & 4.5 Tesla at 4K, 10K & 20K respectively; the same is increased up to 13.5, 11.3 & 5.5 Tesla for the 3-wt% *n*-Diamond added sample, reveals that nano diamond doping significantly improved the H_{irr} values. These results show that diamond doping enhances the flux pinning strength in parent MgB₂ significantly. These results are in well agreement with previously reported data [16].

Using $M(H)$ loop we estimated the critical current density by invoking Bean's critical state formula. Fig. 3 shows the magnetic critical current density (J_c) vs applied field (H) at 20K & 10K. For all the samples (doped and undoped) the J_c attains the value greater than 10^5 A/cm² at low fields at both the temperatures. At 20K J_c falls to 100 A/cm² at 4.5 Tesla for pure MgB₂ whereas for rest of the samples this J_c value is reached only at nearly 6 Tesla. At 20 K the J_c is improved by an order of magnitude for doped samples as compared to the pure MgB₂ at high fields but for doped samples all the plots are merging nearly at the same field (6 Tesla) i.e. not much difference in $J_c(H)$ behavior is seen for doped samples at higher fields. For 10K the situation is quite different at higher fields i.e. the rate of J_c drop is smaller than for all samples compared to undoped MgB₂. The J_c is 40 times higher than pure MgB₂ at 10K at 6 Tesla applied field in case of 3-wt% *n*-Diamond added sample and J_c value is still of the order of 10^3 A/cm² at 10 Tesla for the same sample. These results are quite comparable as reported earlier [17]. The

better $J_c(H)$ performance of n -Diamond added samples indicates towards that the additional impurities at nanoscale introduced by n -Diamond serve as strong pinning centers to improve flux pinning in higher applied fields.

To confirm the improved flux pinning behavior through diamond doping, the field dependence of normalized flux pinning force ($F_p / F_{p, max}$) is shown in fig. 4(a) & (b) at 20K & 10K. The relationship between flux pinning force and critical current density could be described by [18]

$$F_p = \mu_0 J_c(H) H \quad (1)$$

Where μ_0 is the magnetic permeability in vacuum. These figures depict that the pinning forces are significantly improved than the pure MgB₂ above 2 Tesla for n -Diamond doped samples at both the temperatures because curves for the doped samples are shifted towards the higher fields, indicating enhanced flux pinning force in high fields. As revealed by the microstructure analysis [15] *nano* diamond particles of size around ~ 10 nm are dispersed in MgB₂ matrix. Because these particles have the size comparable to the coherence length of MgB₂, It is highly possible that they may work as point pinning centers, causing a shift of the curve in $F_p / F_{p, max}$ vs H curve towards the higher field. It can be seen from fig. 4(a) & (b) that the peak corresponding to 3-wt% n -Diamond doped sample is much broader than those of other samples, indicating highest pinning strength in this sample at higher fields; which is consistent with the results of J_c (fig. 3).

IV. CONCLUSIONS

In summary, the effect of *nano* diamond doping on critical temperature (T_c), critical current density (J_c) and flux pinning was investigated under a wide range of magnetic field. It was found that the n -Diamond addition enhances the flux pinning with modest reduction of the T_c . J_c was enhanced by a factor of 40 in comparison to undoped sample for 3-wt% n -Diamond added sample at 10K at 6 Tesla. The H_{irr} values for the undoped samples are 7.5, 6.5 & 4.5 Tesla at 4K, 10K & 20K respectively; the same is increased up to 13.5, 11.3 & 5.5 Tesla for the 3-wt% n -Diamond added sample. The highly dispersed nano diamond particles are acting as strong pinning centers and are responsible for better performance of doped samples. The present work shows that *nano* diamond doping is a promising way to fabricate high performance MgB₂ bulk material with excellent values of $J_c(H)$, H_{c2} & $H_{irr}(T)$.

ACKNOWLEDGEMENT

Dr. Rajeev Rawat from *CSR-Indore* is acknowledged for the resistivity under magnetic field measurements. Mr. Kranti Kumar and Dr. A. Banerjee are acknowledged for the high field magnetization measurements. Further *DST*, Government of India is acknowledged for funding the 14 Tesla-PPMS-VSM at CSR, Indore. The authors from NPL would like to thank Dr. Vikram Kumar (DNPL) for his great interest in present.

REFERENCES

1. S. X. Dou, W. K. Yeoh, J. Horvat and M. Ionescu, *Appl. Phys. Lett.* **83**, 4996 (2003)
2. R. H. T. Wilke, S. L. Bud'ko, P. C. Canfield and D. K. Finnemore, *Phys. Rev. Lett.* **92**, 217003 (2004)
3. S. X. Dou, O. Shcherbakova, W. K. Yeoh, J. H. Kim, S. Soltanian, X. L. Wang, C. Senatore, R. Flukiger, M. Dhalle, O. Husnjak and E. Babic, *Phys. Rev. Lett.* **98**, 097001 (2007)
4. Y. Ma, H. Kumakura, A. Matsumoto, H. Hatakeyama and K. Togano, *Supercond. Sci. & Tech.* **16**, 852 (2003)
5. S. Y. Li, Y. M. Xiong, W. Q. Mo, R. Fan, C. H. Wang, X. G. Luo, Z. Sun, H. T. Zhang, L. Li, L. Z. Cao and X. H. Chen, *Physica C* **363**, 219 (2001)
6. J.Y. Xiang, D.N. Zheng, J.Q. Li, S.L. Li, H.H. Wen and Z.X. Zhao, *Physica C* **386**, 611 (2003)
7. J. H. Kim, S. Zhou, M. S. A. Hossain A. V. Pan and S. X. Dou, *Appl. Phys. Lett.* **89**, 142505 (2006)
8. J. H. Kim, S. X. Dou, M. S. A. Hossain, X., Xu, J. L. Wang, D. Q. Shi, T. Nakane and H. Kumakura, *Supercond. Sci. & Tech.* **20**, 715 (2007)
9. T. M. Shen, G. Li, X. T. Zhu, C. H. Cheng and Y. Zhao, *Supercond. Sci. & Tech.* **18**, L49 (2005)
10. Arpita Vajpayee, V.P.S. Awana, S. Balamurugan, E. Takayama-Muromachi, H. Kishan and G.L. Bhalla, *Physica C*, In Press (2007)
11. M. Nishiyama, G. Kinoda, Y. Zhao, T. Hasegawa, Y. Itoh, N. Koshizuka and M. Murakami, *Supercond. Sci. & Tech.* **17**, 1406 (2003)
12. C. Krutzler, M. Zehetmayer, M. Eisterer, H. W. Weber, N. D. Zhigadlo, J. Karpinski and A. Wisniewski, *Phys. Rev. B* **74**, 144511 (2006)
13. M. Angst, S. L. Bud'ko, R. H. T. Wilke and P. C. Canfield, *Phys. Rev. B* **71**, 144512 (2005)
14. S. Lee, T. Masui, A. Yamamoto, H. Uchiyama and S. Tajima, *Physica C* **397**, 7 (2003)
15. Arpita Vajpayee, Hannu Huhtinen, V.P.S. Awana, Anurag Gupta, Rajeev Rawat, N.P. Lalla, H. Kishan, R. Laiho, I. Felner and A.V. Narlikar, *Supercond. Sci. & Tech.* **20**, S155 (2007)
16. C. H. Cheng, H. Zhang, Y. Zhao, Y. Feng, X. F. Rui, P. Munroe, H. M. Zheng, N. Koshizuka, and M. Murakami, *Supercond. Sci. & Tech.* **16**, 1182 (2003)
17. C. H. Cheng, Y. Yang, P. Munroe and Y. Zhao, *Supercond. Sci. & Tech.* **20**, 296 (2007)
18. E. Martinez, P. Mikheenko, M. Martinez-lopez, A. Millan, A. Bevan and J. S. Abell, *Phys. Rev. B* **75**, 134515 (2007)

FIGURE CAPTIONS

Figure 1. Superconducting transition zone of Resistance vs Temperature plot under applied magnetic field $R(T)H$ up to 8 Tesla for pure, 5-wt% & 10-wt% *nano* diamond added samples

Figure 2. Magnetization loop $M(H)$ at 10K for MgB_2-nD_x ($x=0\%$, 1%, 3%, 5%, 7% & 10%) up to 12 Tesla field and inset shows the behavior of irreversibility field H_{irr} with respect to *n*-Diamond concentration at 4K, 10K & 20K

Figure 3. Critical current density (J_c) variation with respect to applied magnetic field (H) (a) at 20K & (b) at 10K

Figure 4. Variation of reduced flux pinning force ($F_p/F_{p,max}$) with magnetic field for MgB_2-nD_x ($x=0\%$, 1%, 3%, 5% & 10%) at 20K & 10K

Fig.1

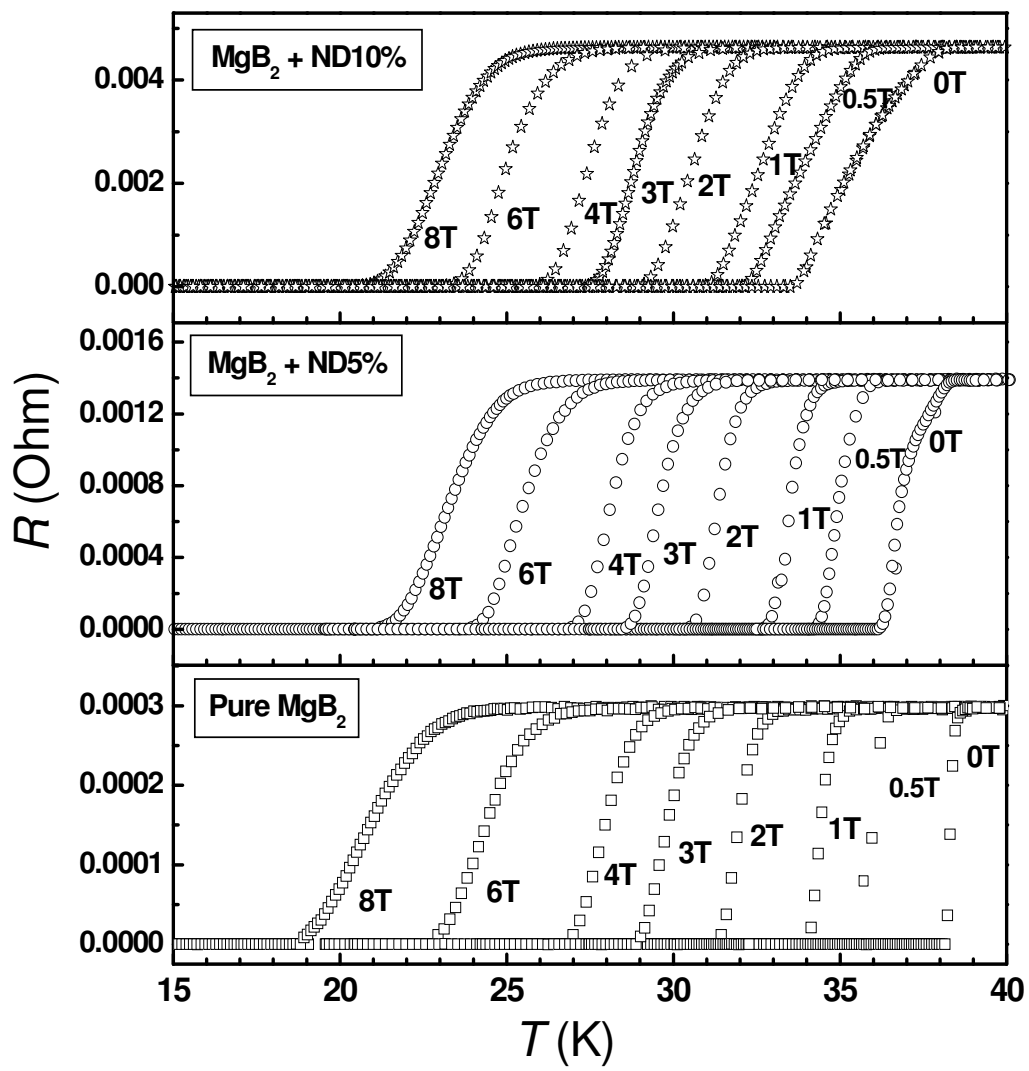


Fig. 2

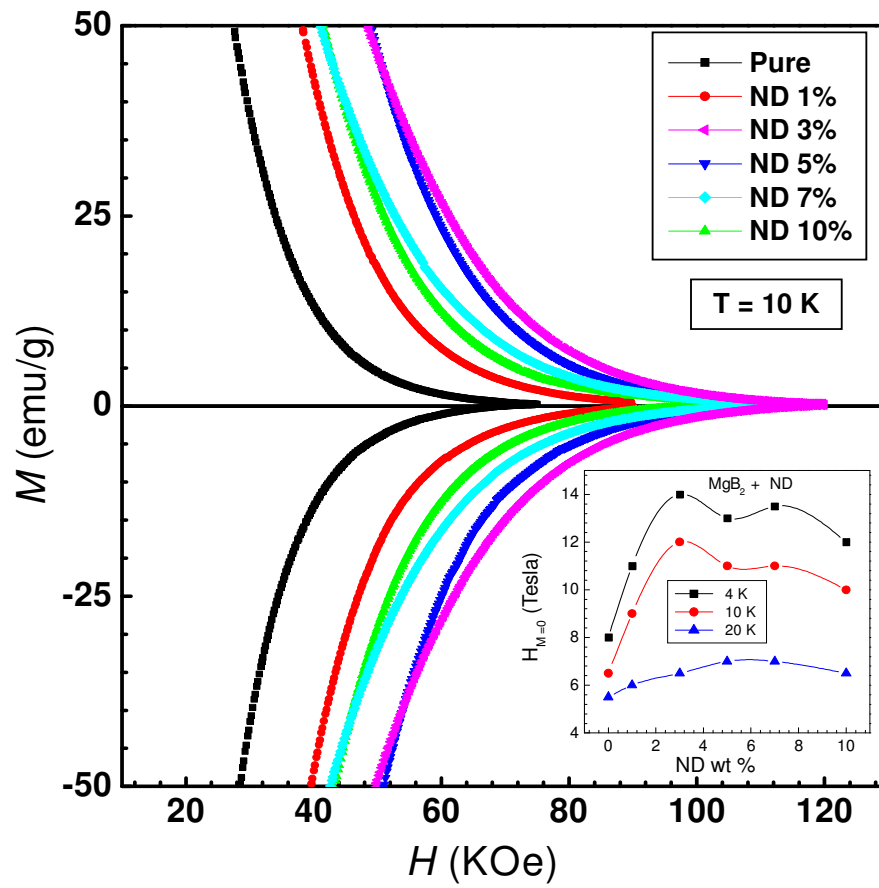


Fig. 3(a) & 3(b)

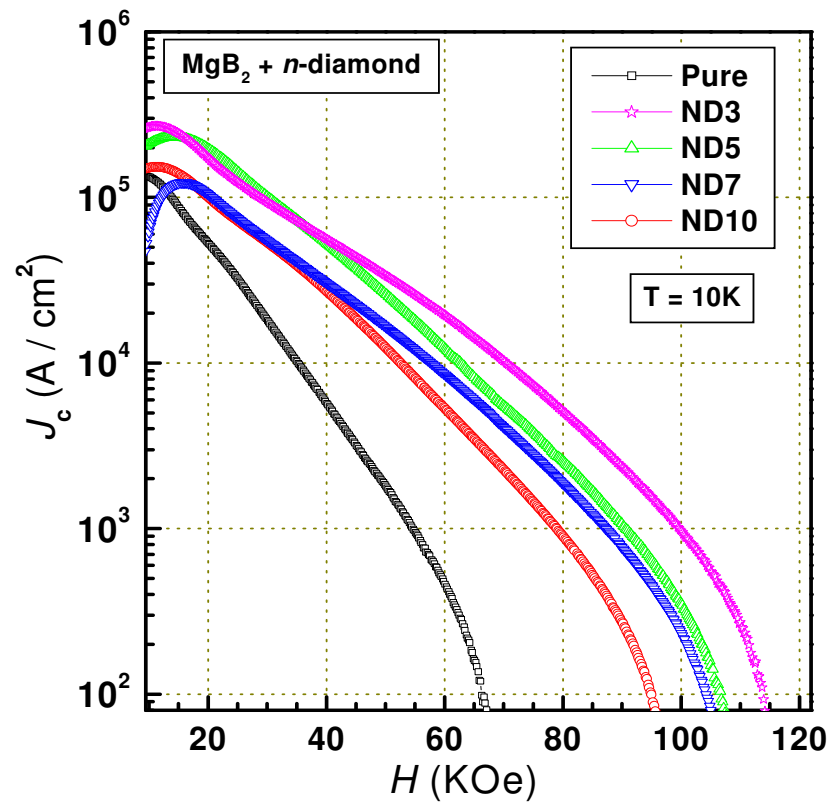
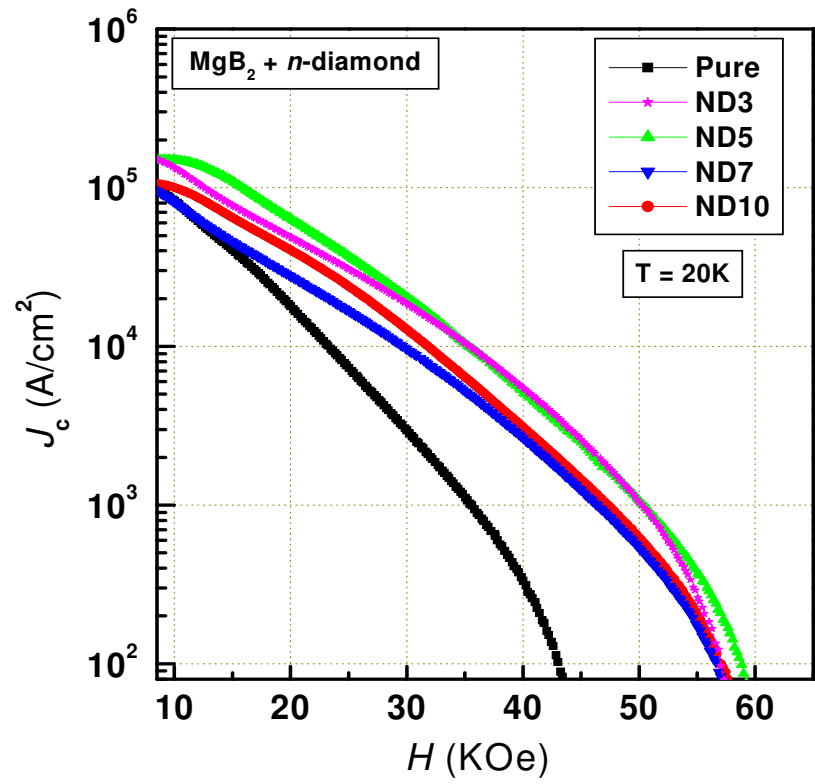


Fig. 4(a) & 4(b)

